Acta Chemica Scandinavica, 1993: 47: 1063–1070
Printed in Belgium – all rights reserved

ACTA
CHEMICA SCANDINAVICA
ISSN 0904–213X

AC Impedance of the Amalgamated Zinc Electrode

Elisabet Ahlberg* and Helge Anderson

Department of Inorganic Chemistry, Chalmers University of Technology and University of Göteborg, S-412 96 Göteborg, Sweden

Ahlberg, E. and Anderson, H., 1993. AC Impedance of the Amalgamated Zinc Electrode. – Acta Chem. Scand. 47: 1063–1070. © Acta Chemica Scandinavica 1993.

The dissolution kinetics of amalgamated zinc has been studied by impedance spectroscopy. A single relaxation is observed in the complex impedance diagram. Two plausible mechanisms are considered, the one-step two-electron transfer and the two-step consecutive mechanism with one adsorbed intermediate. The impedance behaviour of these mechanisms was simulated and compared to the experimental results. For the two-electron transfer mechanism a good agreement between experimental and theoretical data is observed at anodic potentials. However, in the cathodic region a disagreement occurs, and the reason for this is discussed. For the two-step mechanism, with the first step in equilibrium, it was shown that, if this mechanism prevails, the single relaxation observed descends from the intermediate adsorbed on the surface. This is due to the fact that the charge-transfer resistance becomes negligible compared to the polarisation resistance when the first step is in pseudo equilibrium. The potential dependencies of the time constants involved are discussed.

The dissolution kinetics of amalgamated zinc has been studied in great detail by numerous investigators.[1–9] Most of these investigators support the idea that the reaction takes place in two consecutive steps where the first step is in equilibrium. The intermediate is a monovalent species that is adsorbed on the surface, and it is assumed not to be stable in solution.

Impedance spectroscopy (IS) has frequently been used for dissolution and deposition reactions of both pure[10–13] and amalgamated[1–3,8,9,14] metals. One advantage of this technique is the possibility to distinguish relaxation processes with different time constants taking place at the surface. It has been shown that potential-dependent adsorption of intermediates may be responsible for such a relaxation. By using ordinary rate laws for electrochemical reactions it is also possible to show that a sine-wave perturbation of the potential, under certain conditions, may generate pseudo capacitances or even inductances for reactions involving adsorbed intermediates.[15]

The conditions for the occurrence of these effects have been discussed,[16,17] and it can be shown that for a two-step consecutive mechanism with the first step in equilibrium, as proposed in the literature for the dissolution of amalgamated zinc, two relaxations are expected in the impedance spectra, one from the charge-transfer through the double-layer and one from the intermediate adsorbed on the electrode surface. However, experimental results from earlier impedance studies of this reaction reveal only one relaxation in the anodic regime. A possible explanation for this might be that the reaction proceeds via a one-step two-electron transfer. Other explanations can be found in terms of certain conditions under which the consecutive mechanism only reveals one relaxation, although the first step is in equilibrium. These are as follows. (1) The rate of the charge-transfer is very low. The relaxation of the adsorption may then fall outside the frequency region used experimentally. (2) One of the steps is very fast compared to the other. (3) Both reaction steps take place at irreversible potentials. (4) Both time constants are for some reason of similar order.

Since IS studies of the anodic dissolution of amalgamated zinc have shown only one relaxation, one or several of the special cases outlined above should prevail. In this paper we will show that if the consecutive mechanism is correct, the charge-transfer resistance, R_{ct}, must be small compared to the polarisation resistance, R_p. In that case, this will result in a new interpretation of the impedance spectra of this reaction. The relaxation observed is not due to the charge-transfer but instead it reflects the adsorption kinetics of the adsorbed intermediate.

The arguments for this interpretation are based on the results from IS measurements on amalgamated zinc electrodes at different potentials in 2 M $NaClO_4$, pH 3.0. The experimental results are compared to simulations of both the one-step mechanism and the consecutive two-step mechanism which, according to the literature, seem to be the most plausible mechanisms.

* To whom correspondence should be addressed.

List of symbols

α_i	transfer coefficient for the ith reaction step
b_i	$(1-\alpha_i)\,zF/RT$
b_{-i}	$-\alpha_i zF/RT$
β	maximum surface concentration of the adsorbed species
C_{dl}	double-layer capacitance
E	potential
F	Faraday constant
I	current density
I_a	anodic current density
I_c	cathodic current density
I_{ss}	steady state current density
j	complex unit, $\sqrt{-1}$
k_i°	rate constant at equilibrium potential for the ith reaction step
k_i	rate constant for the ith reaction step
K_i°	normalized rate constant at equilibrium potential for the ith reaction step
K_i	normalized rate constant for the ith reaction step
θ	fraction coverage by adsorbed intermediate
θ_{ss}	fraction coverage by adsorbed intermediate at steady state
R_{ct}	charge-transfer resistance
R_p	polarization resistance
τ_{ad}	time constant of the relaxation by adsorbed intermediate as defined from eqn. (6)
τ_{ad}^*	apparent time constant of the relaxation by adsorbed intermediate as defined from eqn. (7)
$\tau_{\omega_{max}}$	time constant as defined from the maximum of the impedance plot in the complex impedance plane
ω	angular frequency, $2\pi f$
Z_F	faradaic impedance
Z_I	interfacial impedance
z	number of electrons transferred

Experimental

Instrumentation, cells and electrodes. A PAR (Princeton Applied Research) 173 potentiostat with a model 276 interface and a HP 85B computer, printer and plotter were used for generation and recording of polarisation curves. A Solartron 1174 frequency response analyser coupled to the PAR potentiostat was used for the impedance measurements. Serious phase shifts in the high-frequency region could be avoided by applying the procedure proposed by Kendig *et al.*[18] Programs for measuring the impedance were developed.[19] Ohmic compensation was achieved by measuring the ohmic resistance between the working electrode and the reference electrode by impedance measurements. Data were mathematically compensated for *iR*-drop on plotting.

The cell was a Metrohm titration vessel with a specially designed lid. A calomel reference electrode with saturated NaCl solution, SSCE ($E = 0.236$ V vs. NHE), and a platinum counter-electrode were used throughout the work. The counter electrode was separated from the electrolyte to avoid contamination. The electrolyte solution was bubbled with purified nitrogen for at least 40 min before the experiment was started, and a nitrogen atmosphere was maintained in the cell during the experiments.

Rotating-disc electrodes with a surface of 0.2 cm^2 were prepared from 99.99% pure zinc rods (Johnson Matthey Chemicals Ltd.). The electrodes were moulded in epoxy, exposing only the circular disc surface. Before the amalgamation of the electrode, it was wet-ground on silicon carbide paper (1000 and 4000 mesh), rinsed with doubly distilled water and immediately placed in 0.5 M $HClO_4$ for a short time. The amalgamation of the electrode was carried out by immersion in 10 mM $Hg(NO_3)_2 + 0.5$ M $HClO_4$ solution for 20 min. This procedure resulted in a shiny film on the electrode. The film was allowed to saturate for 1 h in 0.5 M $HClO_4$ solution before it was placed in the cell. The rotating speed of the electrode was 50 r.p.s. in all experiments. The current was found to be independent of the rotation speed of the electrode in the range 30–90 r.p.s. This indicates kinetic behaviour for both the anodic and the cathodic reaction.

Chemicals. 2 M sodium perchlorate was prepared from p.a. $NaClO_4$ (Merck) and doubly distilled water. The pH of the solution was adjusted by addition of perchloric acid or sodium hydroxide of the same ionic strength as the electrolyte. The pH was controlled by a pH-stat system from Radiometer (pH meter 84, titrator TTT 80 and autoburette ABU 80) together with a combined glass electrode GK 2401c.

Impedance measurements. The impedance was measured from 100 kHz to 10 mHz with 8 measurements per decade of frequency. Measurements were performed from -900 mV in the anodic region to -1200 mV in the cathodic region. The rest potential in the solution containing 10 mM $Zn(ClO_4)_2$ was stable at -1044 mV within 1 mV.

Polarisation measurements. Each polarisation measurement consisted of three scans with a sweep rate of 2 mV s^{-1}. The first scan started in the anodic direction from the rest potential to -800 mV vs. SSCE, the second from -800 to -1150 mV and the third from -1150 to -800 mV. Hysteresis was negligible.

Simulation of the impedance. The details of the calculations of the impedance function for different mechanisms have been described elsewhere[16] and will briefly be outlined here. The Faradaic current response $\Delta I_f = |\Delta I_f| \exp(j\omega t)$, of the sinusoidal voltage perturbation, $\Delta E = |\Delta E| \exp(j\omega t)$, is obtained from a first-order Taylor expansion of the current expression that describes the flow of charge through the electrode (conservation of charge). For a kinetically controlled process where

Table 1. Parameters used in the simulations of the mechanisms.[a]

Parameter	Mechanism	
	$Zn \rightleftharpoons Zn^{2+}_{aq} + 2e^-$	$Zn \rightleftharpoons Zn^{+}_{ad} + e^-$ $Zn^{+}_{ad} \rightleftharpoons Zn^{2+}_{aq} + e^-$
I (Charge-balance)	$F\{K_1 - K_{-1}\}$	$F\{(K_1 - K_{-2})(1-\theta) + (K_2 - K_{-1})\theta\}$
$\beta\, \partial\theta/\partial t$ (Mass-balance)		$(K_1 + K_{-2})(1-\theta) - (K_2 + K_{-1})\theta\}$
I_{ss}	$F\{K_1 - K_{-1}\}$	$2F\{(K_2\theta_{ss} - K_{-2}(1-\theta_{ss})\}$
θ_{ss}		$\dfrac{K_1 + K_{-2}}{K_1 + K_{-1} + K_2 + K_{-2}}$
$\partial I/\partial E$ ($\theta = \text{const} \Rightarrow \partial I/\partial E = 1/R_{ct}$)	$F\{b_1K_1 - b_{-1}K_{-1}\}$	$F\{b_1K_1 - b_{-2}K_{-2} + (b_2K_2 + b_{-2}K_{-2} - b_1K_1 + b_{-1}K_{-1})\theta_{ss}\}$
$\partial I/\partial E^b$ ($\theta(E) \Rightarrow \partial I/\partial E = 1/R_p$)		$2F\dfrac{A1 + A2 + A3 + A4}{A5}$
$\partial I/\partial\theta$		$F\{K_2 + K_{-2} - K_1 - K_{-1}\}$
$\Delta\theta/\Delta E$		$\dfrac{b_1K_1 + b_{-2}K_{-2} - (b_2K_2 + b_{-2}K_{-2} + b_1K_1 + b_{-1}K_{-1})\theta_{ss}}{K_1 + K_{-1} + K_2 + K_{-2} + j\omega\beta}$
τ_{ad}		$\dfrac{\beta}{K_2 + K_{-2} - K_1 - K_{-1}}$
$\tau^*_{ad}{}^c$		$\dfrac{1}{(1/\tau_{ad}) + R_{ct}B}$

[a] K_i indicates a normalized rate constant, which is the rate constant k_i multiplied by the concentration of the reacted species. [b] $A1 = b_1K_1[K_2(K_{-1} + K_2 + K_{-2}) + K_{-1}K_{-2}]$, $A2 = b_2K_2[K_1(K_1 + K_{-1} + K_{-2}) + K_{-1}K_{-2}]$, $A3 = b_{-1}K_{-1}[K_{-2}(K_1 + K_2 + K_{-2}) + K_1K_2]$, $A4 = b_{-2}K_{-2}[K_{-1}(K_1 + K_{-1} + K_2) + K_1K_2]$, $A5 = (K_1 + K_{-1} + K_2 + K_{-2})^2$. [c] $B = \partial I/\partial\theta\ \partial(d\theta/dt)/\partial E$.

one adsorbed intermediate is present, the Faradaic impedance, Z_F, may then be written as eqn. (1), where $\Delta\theta$

$$\frac{1}{Z_F} = \frac{\Delta I}{\Delta E} = \frac{1}{R_{ct}} + \frac{\partial I}{\partial\theta}\frac{\Delta\theta}{\Delta E} \tag{1}$$

is obtained from the Taylor expansion of the time dependence of the coverage of the adsorbed intermediate (conservation of mass).

By making assumptions concerning the adsorption of intermediates and the rate of the electron transfer, and by using the definition of the interfacial impedance (2), the quantities necessary for the determination of the impedance can be evaluated. The adsorption of intermediates is assumed to follow the Langmuir adsorption isotherm and the rate of the electron transfer is exponentially related to the potential in the usual way. If no intermediates are present, the last term disappears and the faradaic impedance is equal to the charge transfer resistance, R_{ct}. The interfacial impedance is obtained by taking the electrical double layer into account, regarding it as a pure capacitor with the capacitance, C_{dl}, parallel to the faradaic impedance. The interfacial impedance, Z_I, can thus be written as eqn. (2).

$$\frac{1}{Z_I} = \frac{1}{R_{ct}} + \frac{\partial I}{\partial\theta}\frac{\Delta\theta}{\Delta E} + j\omega C_{dl} \tag{2}$$

The quantities in this expression may be obtained from the mass and charge balance equations for the mechanism of interest (Table 1). The rate constants and the other parameters used in the simulations are listed in Table 2. The value of β needs some comments. It corresponds to the maximum concentration of the adsorbed intermediate and is usually set to the concentration of one monolayer ($\approx 3 \times 10^{-9}$ mol cm^{-2}). The solubility of zinc in mercury is approximately 6 at. %,[20] which means that a maximum concentration of 1.8×10^{-10} mol cm^{-2} is expected. Thus a low value of β has been used in the calculations.

Table 2. Numerical values of the parameters used in the simulations.

Mechanism	n	K°_n/ mol cm^{-2} s^{-1}	K°_{-n}/ mol cm^{-2} s^{-1}	α_n	β/ mol cm^{-2}	E°/ mV	C_{dl}/ μF
One step	1	1.42×10^{-9}	1.58×10^{-9}	0.5		−1050	20
Consecutive	1	1.74×10^{-6}	2.20×10^{-5}	0.5	10^{-10}	−1025	20
	2	3.09×10^{-8}	4.34×10^{-10}	0.5			

Results and discussion

Typical experimental impedance plots are shown in Fig. 1. The corresponding potential dependence of the steady-state current, I_{ss}, polarisation resistance, R_p, and the time constant, τ, of the single relaxation observed are shown in Fig. 2. The slopes of the plots are 56, −65 and −54 mV, respectively, in the anodic potential region, and −113, 134 and 232 mV, respectively, in the cathodic potential region.

It was found that the electrode became over-saturated with zinc during the relatively long impedance measurements (40 min) in the cathodic potential region. Thus the electrode could not be regarded as amalgamated during these measurements. In an attempt to reduce this problem, potentiodynamic sweeps with a sweep rate of 2 mV s^{-1} were performed. The Tafel slope at anodic potentials was the same as in the steady state measurements (52–56 mV), and in the cathodic potential region Tafel slopes between −106 and −117 mV were obtained. Fig. 3 shows the polarisation curves in the cathodic region as a function of zinc ion concentration. The reaction order of the cathodic reaction with respect to zinc ions was found to be 0.93. However, the state of the electrode during these measurements, amalgamated or not, is still uncertain. This will be considered later.

In the literature the cathodic Tafel slope for amalgamated zinc has a value close to −120 mV, while for the reduction of zinc on mercury lower values are found, about −60 mV. The same trend has also been observed in the studies of copper ion reduction.[21] The conclusion drawn from that paper was that the reduction of Cu^{2+} proceeds in two steps via an adsorbed intermediate at amalgamated electrodes, whereas the electron transfer takes place in a single step on pure mercury electrodes. This description can be used for the reduction of zinc as pointed out by Sierra.[14] A simple explanation of the quantum-mechanically improbable two-electron transfer on pure mercury could be that the liquid surface is not able to stabilise the intermediate long enough to separate the electron transfers into two steps.

The simulated results from the single step mechanism [1] are rather straight forward, as shown by reaction (3).

$$Zn \underset{k_{-1}}{\overset{k_1}{\rightleftharpoons}} Zn^{2+}_{aq} + 2e^- \qquad (3)$$

The polarisation resistance will be equal to the charge-transfer resistance for all potentials. The Tafel slopes of

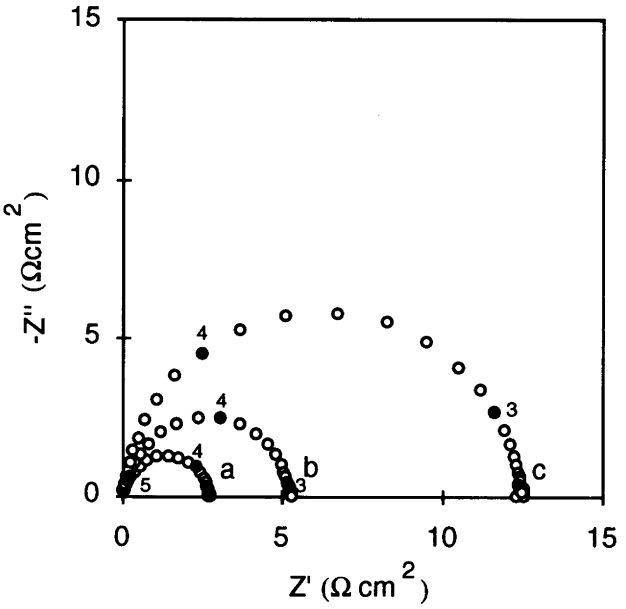

Fig. 1. Impedance spectra for the amalgamated zinc electrode in 2 M $NaClO_4$ + 0.01 M $Zn(ClO_4)_2$, pH 3.0 at three anodic potentials. (a) −962, (b) −982 and (c) −1002 mV vs. SSCE. The numbers on the spectra indicate the logarithm of the angular frequency, ω.

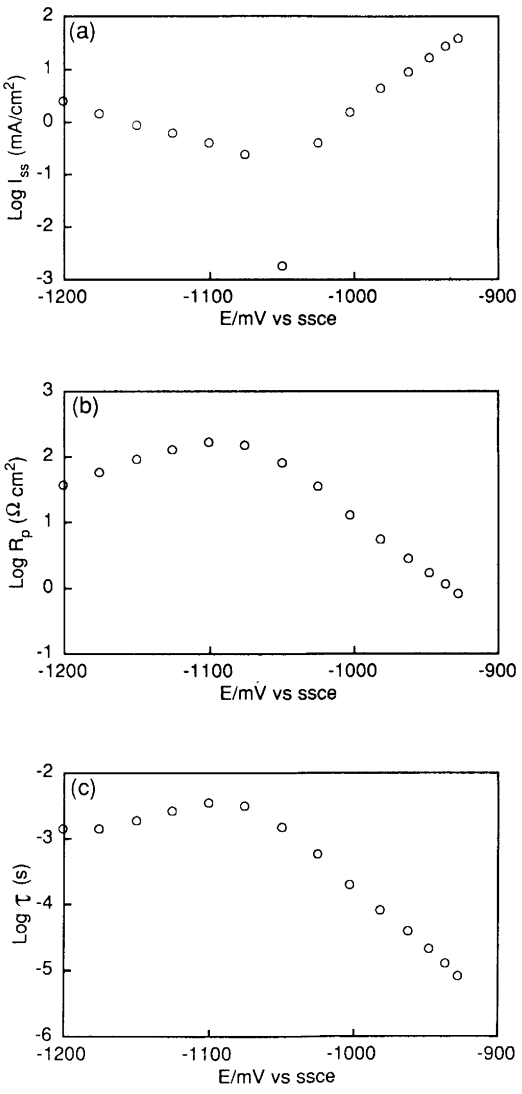

Fig. 2. Potential dependences of (a) the steady-state current, (b) the polarisation resistance and (c) the time constant for the amalgamated zinc electrode in 2 M $NaClO_4$ + 0.01 M $Zn(ClO_4)_2$, pH 3.0.

the anodic and cathodic reactions are 60 and -60 mV, respectively. The corresponding experimental values obtained are 52–56 mV for the anodic process and -106 to -117 mV for the cathodic process. In Fig. 4 the logarithm of the steady-state current density, $\log I_{ss}$, $\log R_p$ and $\log \tau_{\omega_{max}}$ are plotted as functions of the potential together with the experimental data. A good correlation is achieved between the simulated data and the experimental data in the anodic potential region, while there is a disagreement for the cathodic potentials. The poor agreement at cathodic potentials may be explained by the possibility of crystallisation of Zn on the electrode as mentioned above.

Simulating the consecutive mechanism, reactions (4) and (5), with the first step in pseudo-equilibrium usually

$$Zn \underset{k_{-1}}{\overset{k_1}{\rightleftharpoons}} Zn_{ad}^{+} + e^{-} \quad (4)$$

$$Zn_{ad}^{+} \underset{k_{-2}}{\overset{k_2}{\rightleftharpoons}} Zn_{aq}^{2+} + e^{-} \quad (5)$$

reveals two relaxations. However, it is possible to generate impedance spectra of this mechanism with the first step in equilibrium which reveal only one loop in the impedance plane. As described earlier, four conditions can be classified which generate these spectra. (1) The rate of the charge-transfer is very low, which may cause the time constant of the relaxation of the intermediate to fall outside the low-frequency part of the spectrum. (2) The rate of one step is very high compared to the other step. This makes R_{ct} very small compared to R_p, and the relaxation from the intermediate will be the only part visible. (3) The reaction is totally irreversible. (4) The maximum available surface for the intermediate, β, is very low, which may reduce the time constant of the adsorbed intermediate and thus interfere with the relaxation from charge-transfer through the double layer.

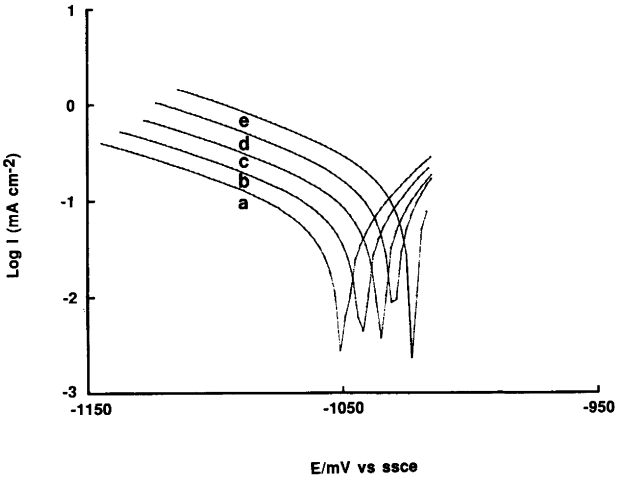

Fig. 3. Cathodic polarisation curves for the amalgamated zinc electrode in 2 M $NaClO_4$, pH 3.0 at five different zinc ion concentrations: (a) 0.010, (b) 0.018, (c) 0.032, (d) 0.056 and (e) 0.100 M.

If the consecutive mechanism is to be regarded as possible, at least one of the above mentioned conditions must prevail.

It was found that the simulation of the consecutive mechanism did not yield a satisfactory value of the corresponding steady-state current when R_{ct} was fitted to the low-frequency experimental data, except when the difference between R_{ct} and R_p was small. However, a small difference between R_{ct} and R_p is not compatible with the first step in equilibrium and the low Tafel-slope obtained experimentally. If instead R_p was fitted to the impedance of low frequencies, a much better correlation between the steady-state current and the low-frequency impedance was obtained. The latter indicates that, if the consecutive mechanism prevails, the impedance at low frequencies reflects the polarisation resistance, which differs considerably from the charge-transfer resistance when the

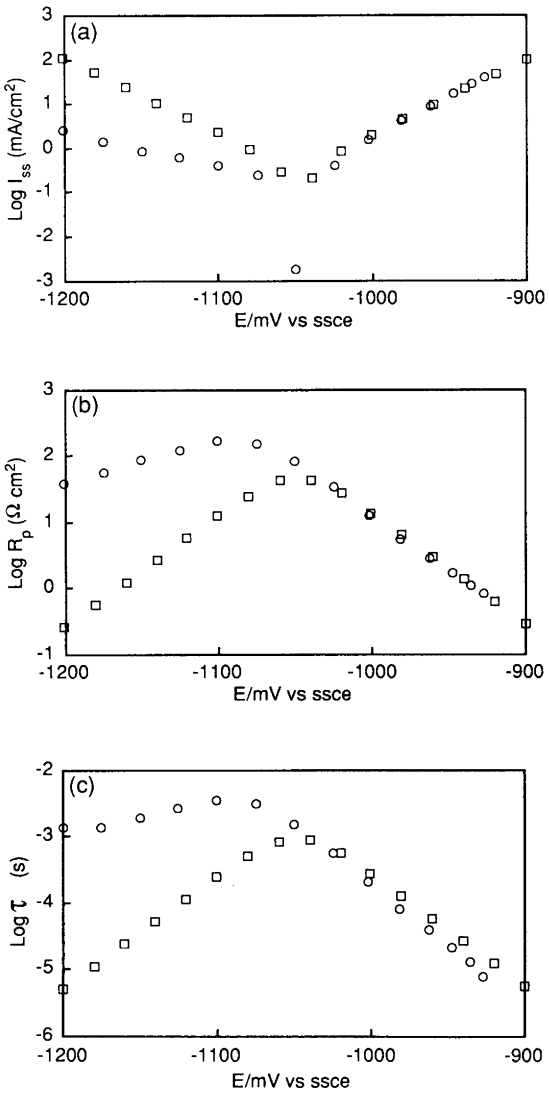

Fig. 4. Potential dependences of (a) the steady-state current, (b) the polarisation resistance and (c) the time constant for the one-step mechanism; (○) experimental data, (□) simulated data.

first step is in equilibrium. So far, the simulations still yield two relaxations, a result which contradicts the experiments. The possibilities of a single relaxation in the case of the consecutive mechanism with the first step in equilibrium, listed above, may therefore be viewed in closer detail. The first point (high R_{ct}) can be ruled out by noting that if R_{ct} is fitted to the experimental low-frequency data, the only way to make the time constant of the adsorbed intermediate to fall outside the measured frequency range is to use a β-value that corresponds to an adsorption layer of the monovalent intermediate that is far too thick (approximately 100 monolayers). This is not realistic. The third explanation can be eliminated, since it can be shown that the product of $\partial I/\partial\theta$ and $\Delta\theta/\Delta E$ is low ($R_{ct} \approx R_p$) only at irreversible potentials far from the equilibrium potential, which in turn should give a 120 mV anodic Tafel slope. The fourth possibility (low β) was simulated in the anodic potential region with the time constants from both relaxations approximately of the same order. It was found that the impedance spectra showed a clear distortion from the semi-circle and that the distortion varied with the potential. The experimental semi-circles (Fig. 1) do not show any distortion of this kind.

The second point above (a fast first step and low R_{ct}) contradicts neither the experiments nor the theoretical considerations. Fig. 5 shows the simulated results together with the experimental data. The rate of the first step was approximately two decades in magnitude higher than the second step at the equilibrium potential, E^0. A much better correlation is now obtained for both the steady-state current and the polarisation resistance. The polarisation resistance is about 400 times higher than the charge-transfer resistance at the rest potential, which

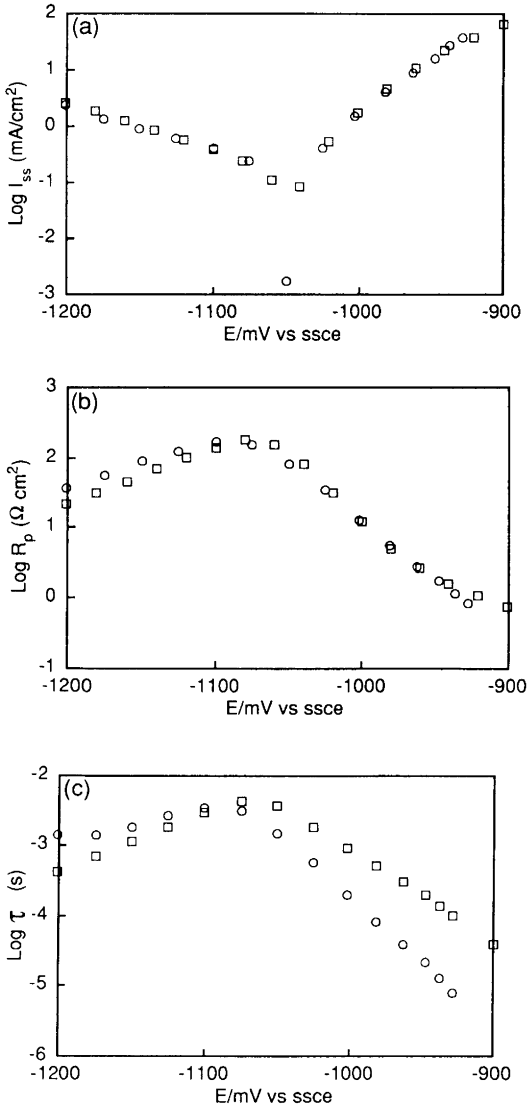

Fig. 5. Potential dependences of (a) the steady-state current, (b) the polarisation resistance and (c) the time constant for the two-step mechanism; (○) experimental data, (□) simulated data.

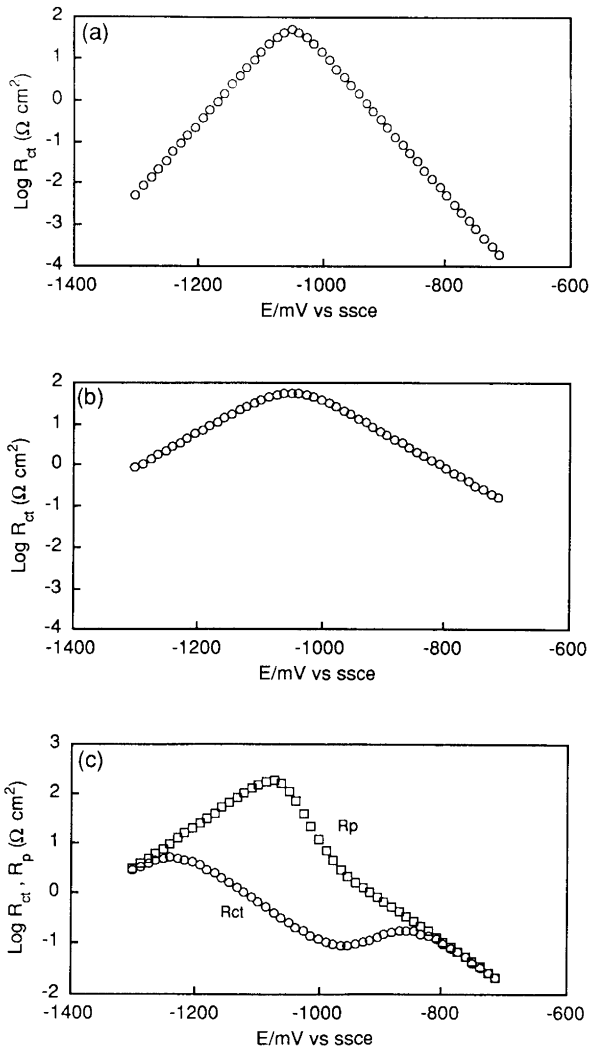

Fig. 6. Simulated potential dependences of R_{ct} and τ_{ct}: (a) single-step mechanism, (b) two-step mechanism with the first step rate-determining and (c) two-step mechanism with the first step in equilibrium.

explains the absence of the charge-transfer loop. The time constant of the adsorbed intermediate does not, on the other hand, correlate very well with the experimental time constants, which of course must be considered. It is therefore worth pointing out the behaviour of the time constants in the potential domain, as predicted by the two mechanisms considered here.

The time constant for the transfer of charge through the double layer, τ_{ct}, is simply the product of R_{ct} and the double-layer capacity, C_{dl}. Since C_{dl} is considered to be independent of the potential in the simulations, the time constant of the charge-transfer process is proportional to R_{ct}. In Fig. 6 the potential behaviours of log R_{ct} [and R_p, Fig. 6(c)] for the two mechanisms are plotted. The two-electron transfer, Fig. 6(a), shows the expected slopes of ± 60 mV. Figs. 6(b) and 6(c) show the plot of log R_{ct} and R_p for the consecutive mechanism when the first step is slow and rate determining (b), and when it is fast and in equilibrium (c). In the first case R_{ct} and R_p coincide, and no relaxation of the intermediate will be seen in the spectra. The slopes are ± 120 mV. In Fig. 6(c) it can be seen that when the first step is in equilibrium ($k_1 \approx k_{-1} \approx 100\,k_2 = 100\,k_{-2}$ at E^0) the plot of log R_{ct} (and thus log τ_{ct}) contains a dip in the potential region around the equilibrium potential. As the first step in the consecutive mechanism is increased compared to the second step, this dip will be deeper, which means that the difference between R_{ct} and R_p will increase. The slopes of log R_{ct} and log τ_{ct} vs. the potential are ± 120 mV in the linear regions. The log R_p curve is inversely related to the logarithm of the steady-state curve, and the slopes are therefore the same as the Tafel slopes, but with opposite signs, -40 or ± 120 mV.

With the adoption of the consecutive mechanism and with the first step in equilibrium, the predicted reverse behaviour of τ_{ct} (and R_{ct}) in the vicinity of E^0 supports the idea that the visible relaxation in the spectra is a result of the adsorption process. As far as we know, this reverse behaviour has not been reported experimentally.

The potential dependence of the time constant associated with the intermediate, τ_{ad}, can be derived from the equations governing the mechanism. It can be shown that for the consecutive mechanism the time constant of the adsorbed intermediate can be expressed as eqn. (6).

$$\tau_{ad} = \beta/(k_1 + k_{-1} + k_2 + k_{-2}) \tag{6}$$

The slope of the linear parts of log τ_{ad} vs. the potential should be ± 120 mV. However, τ_{ad} does not necessarily

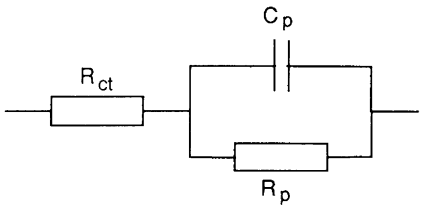

Fig. 7. Equivalent circuit that describes the faradaic impedance for a two-step mechanism.

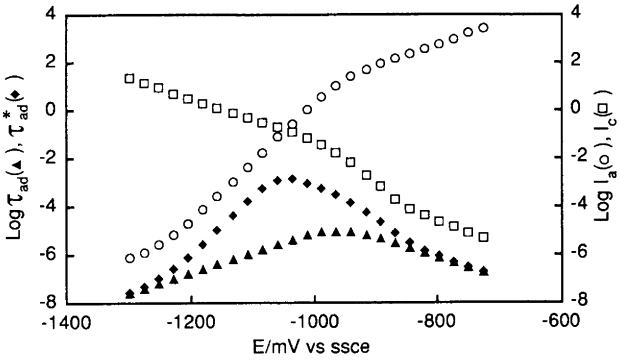

Fig. 8. Simulated potential dependences of the time constants, τ_{ad} and τ^*_{ad}, and the anodic and cathodic steady state current, I_a and I_c, in the two-step mechanism: (▲) log τ_{ad}, (◆) log τ^*_{ad}, (○) log I_a and (□) log I_c.

correspond to the maximum on the semi-circle in the impedance plot. By using a simple equivalent circuit (Fig. 7), originally suggested by Gerischer,[22] to describe the charge-transfer process with one adsorbed intermediate, the quantities in the impedance expression (1) can be identified with the quantities in the expression of the equivalent circuit.[15, 23] This results in the relation† between τ_{ad} and the time constant, τ^*_{ad} shown in eqn. (7),

$$\tau^*_{ad} = \frac{1}{(1/\tau_{ad}) + R_{ct}B} \tag{7}$$

where τ^*_{ad} should correspond to the frequency at the maximum of the semi-circle. B is defined in footnote (c) in Table 1. Fig. 8 shows the potential dependence of log τ^*_{ad} and log τ_{ad}. The difference between the two time constants is enhanced in the same potential region in which R_{ct} differs from R_p. Fig. 8 also shows the potential dependence of the logarithm of the anodic and cathodic currents, I_a and I_c, plotted separately to indicate the close relation between I_a, I_c and τ^*_{ad}. However, comparison between the calculated τ^*_{ad} and the time constant obtained by estimating the angular frequency at the maximum of the simulated spectra showed an unexpected deviation at cathodic potentials. Since we are not able to explain this disagreement, the comparison between experimental and simulated time constants has been carried out by estimating the frequency at the maximum of the impedance curve, $\tau_{\omega_{max}}$, in the complex impedance plane. The estimation was performed by fitting the imaginary part of $Z(\log \omega)$ to a polynomial of third degree.

The interpretation of the results presented here depends on the state of the electrode during the cathodic measurements. The zinc crystallisation that seems to take

† The notation in Ref. 15 is somewhat different than showed here. However, the expression given by Armstrong, $\tau = (1/\omega^*)[(R_0 + R_{ct})/R_0]$, is equivalent to the one given above with the following substitutions: $\omega^* = 1/\tau^*$; $R_0 = 1/\tau B$.

place at cathodic potentials makes it uncertain to analyse the anodic and cathodic data simultaneously with the same mechanism. If only the data from anodic potentials are considered, the single two-electron transfer is the most probable mechanism, since all parameters plotted in Fig. 2 (I_{ss}, R_p and $\tau_{\omega_{max}}$) show a good correlation with the experimental data. Even if I_{ss} and R_p agree very well with simulated data from the two-step mechanism, the potential dependence of $\tau_{\omega_{max}}$ is not good enough to consider the two-step mechanism possible. On the other hand, taking the whole potential region into account, the consecutive mechanism shows a better correlation with the experiments. The distinction between the two mechanisms is hard to make with the experiments reported in this paper. However, a consequence of the present analysis that is important to stress, is that if the consecutive mechanism is assumed, the relaxation observed in the impedance spectra of amalgamated zinc at anodic potentials is caused by the adsorption process of the monovalent intermediate and not by the charge-transfer through the double-layer.

Conclusions

In the present study it is shown that if the dissolution of amalgamated zinc takes place in two consecutive steps the single semi-circle observed in the impedance diagram is due to the adsorption of the intermediate and cannot therefore be regarded as a charge-transfer loop.

The results obtained at anodic potentials indicate that a one-step mechanism for the dissolution process is possible.

At potentials where Zn^{2+} is deposited, it is uncertain whether the electrode is amalgamated or not. No conclusions can therefore be drawn from measurements at cathodic potentials.

Acknowledgment. Financial support from Volvo is gratefully acknowledged.

References

1. Sluyters-Rehbach, M., Ijzermans, A. B., Timmer, B., Griffioen, J. B. and Sluyters, J. H. *J. Electroanal. Chem. 11* (1966) 483.
2. Timmer, B., Sluyters-Rehbach, M. and Sluyters, J. H. *J. Electroanal. Chem. 14* (1967) 181.
3. Van der Pol, F., Sluyters-Rehbach, M. and Sluyters, J. H. *J. Electroanal. Chem. 58* (1975) 177.
4. Baugh, L. M., Tye, F. L. and White, N. C. *J. Appl. Electrochem. 13* (1983) 623.
5. Blackledge, J. and Hush, N. S. *J. Electroanal. Chem. 5* (1963) 435.
6. Blackledge, J. and Hush, N. S. *J. Electroanal. Chem. 5* (1963) 420.
7. Hendrikx, J., Putten, A. v. d., Visscher, W. and Barendrecht, E. *Electrochim. Acta 29* (1984) 81.
8. Hendrikx, J., Visscher, W. and Barendrecht, E. *Electrochim. Acta 30* (1985) 999.
9. Hurlen, T. and Eriksrud, E. *J. Electroanal. Chem. 45* (1973) 405.
10. Keddam, M., Mattos, O. R. and Takenouti, H. *J. Electrochemical Soc. 128* (1981) 257; 266.
11. Ahlberg, E. and Anderson, H. *Acta Chem. Scand. 46* (1992) 15.
12. Macdonald, D. D., Real, S., Smedley, S. I. and Urquidi-Macdonald, M. *J. Electrochem. Soc. 135* (1988) 2410.
13. Cachet, C. and Wiart, R. *J. Electroanal. Chem. 129* (1981) 103.
14. Sierra, A. H. B. and Harrison, J. A. *Electrochim. Acta 22* (1977) 627.
15. Armstrong, R. D. and Henderson, M. *J. Electroanal. Chem. 39* (1972) 81.
16. Ahlberg, E. and Anderson, H. *Acta Chem. Scand. 46* (1992) 1.
17. Bai, L. and Conway, B. E. *J. Electrochem. Soc. 138* (1991) 2897.
18. Kendig, M. W., Allen, A. J. and Mansfeld, F. *J. Electrochem. Soc. 131* (1984) 935.
19. Ahlberg, E. and Friel, M. *Electrochim. Acta 34* (1989) 1523.
20. In *IUPAC Solubility Data Series* (Hirayama, C., Galus, Z. and Guminsti, C., Eds.), Vol. 25, p. 385, Pergamon Press, Oxford 1986.
21. Burrows, I. R., Dick, K. L. and Harrison, J. A. *Electrochim. Acta 21* (1976) 81.
22. Gerischer, H. *Z. Phys. Chem. Leipzig 201* (1952) 55.
23. Cao, C. N. *Electrochim. Acta 35* (1990) 831.

Received February 9, 1993.